PNNL-15453

Pacific Northwest
National Laboratory
Operated by Battelle for the
U.S. Department of Energy

Contamination in LaCl3:Ce Scintillators

B. D. Milbrath
J. I. McIntyre
R. C. Runkle
L. E. Smith

December 2005

Prepared for the U.S. Department of Energy
under Contract DE-AC05-76RL01830

PACIFIC NORTHWEST NATIONAL LABORATORY
operated by
BATTELLE
for the
UNITED STATES DEPARTMENT OF ENERGY
under Contract DE-ACO5-76RLO183O

PNNL-15453

Contamination in LaCl3:Ce Scintillators

B. D. Milbrath
J. I. McIntyre
R. C. Runkle
L. E. Smith

December 2005

Prepared for the U.S. Department of Energy
under Contract DE-AC05-76RL01830

Contamination in $LaCl_3$:Ce Scintillators

PNNL-15453

B.D. Milbrath, J.I. McIntyre, R.C. Runkle, L.E. Smith

Pacific Northwest National Laboratory, MS P8-20, P.O. Box 999, Richland, WA 99352, USA

December 2005

Abstract

We discuss the gamma-, beta-, and x-ray-contamination in $LaCl_3$:Ce scintillators due to the presence of the naturally occurring radioisotope La-138. As the size of lanthanum halide crystals grows towards volumes that are useful in a wider range of applications, and the effect of alpha-contamination due to Ac-227 has been substantially reduced, the effect of La-138 in background and low-count spectra becomes more problematic. For a 38 mm x 38 mm right cylinder detector we found the La-138's x-ray peak had a count rate of 23.8 counts/s and its gamma rays at 789 and 1435 keV caused count rates over 2 counts/s. The effect of this internal contamination will have to be investigated for each potential application. For example, the observed 1435-keV peak interferes with and is larger than the background K-40 1461-keV peak, which could be problematic for handheld detectors. We also look at the crystal's performance in high neutron fluxes, where La-139's large cross section will cause noticeable activation in high neutron fields.

Motivation

In a previous report, we discussed the determination of Ac-227 as the source of alpha-contamination in lanthanum halide crystals [1]. This conclusion was reached independently by others [2], and was in contrast to Saint-Gobain's initial identification of undetermined locations in the U-235 and U-238 decay chains [3,4]. The previous PNNL report also mentioned the presence of naturally-occurring radioisotope La-138 as a gamma- and beta-contaminant, but the extent to which this isotope affects the background and low-count spectra was not readily apparent due to the small crystal sizes (2.0 cm^3 or less) and the large alpha-contamination (0.37-1.8 counts/s/g).

Since our initial study, Saint-Gobain has reduced the alpha-contamination in their lanthanum halide crystals by over two orders of magnitude (as low as 0.005 counts/s/g), apparently by, in part, screening the raw lanthanum materials for uranium background activity [3]. Saint-Gobain has also successfully grown larger crystals and now offers $LaCl_3$:Ce and $LaBr_3$:Ce scintillators (up to 38 mm x 38 mm) for sale [5]. These successes bring the La-138 contamination issue to the forefront.

La-138 decays by both electron capture (66.4%) and beta decay (33.6%). (See Figure 1.) The electron capture produces (100%) a 1435.8-keV gamma ray, often in coincidence with a Ba K x-ray of approximately 31-38 keV. The beta decay (255-keV endpoint) produces (100%) a 788.7-keV gamma ray [6]. These internally emitted cascades can be

problematic or advantageous, depending on the application and the corresponding requirements on the medium-resolution gamma-ray spectrometer systems.

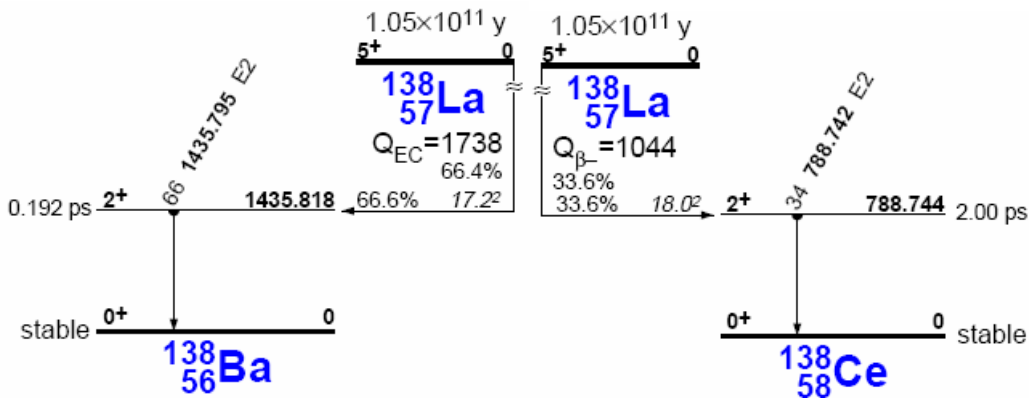

Figure 1. The La-138 decay schemes from ref. [6].

The lanthanum halide scintillators have an energy resolution of 3-4% at 662 keV [7, 8, 9], offering a substantial improvement over NaI(Tl), whose resolution is typically 6-7%. They appear poised to occupy a middle-ground between large, low-resolution scintillators such as NaI(Tl) and CsI, and small, high-resolution solid-state detectors. Thus it is important to understand to what degree the internal contamination found in lanthanum halide scintillators compromises their usefulness.

Investigation of Effects of La-138 Contamination on Spectra

For this study, we obtained a 38 mm x 38 mm right cylinder $LaCl_3$:Ce crystal attached to a Photonis XP2060B photomultiplier tube from Saint-Gobain [10]. Its measured energy resolution at 662 keV (1332 keV) was 4.4% (2.4%). The spectrum from a 50000-second, unshielded background measurement is shown in Figure 2. The alpha contamination is

revealed by the four (one being much smaller than the others) broad peaks in the 1700-3000 keV (gamma-ray calibrated) energy range. (The actual alpha energies are in the range of 5000-7400 keV. Heavy charged particles, such as alphas, produce less light than gamma rays of the same energy.) The count rate in the alpha region for this crystal was 0.011 counts/s/g, an improvement over earlier crystals by a factor of 170. An MCNPx [11] simulation suggested that approximately 40% of the counts in this region were due to background and 60% were due to the alpha contamination. The small, lowest-energy alpha peak was not seen in our earlier studies using lower-resolution crystals. That peak is due to the 1.38% alpha-decay branch of Ac-227 which produces a lower-energy alpha (Q = 5042 keV) [6] than the other alpha-decaying daughters in the chain. This provides direct proof of Ac-227 as the alpha contaminant source [2].

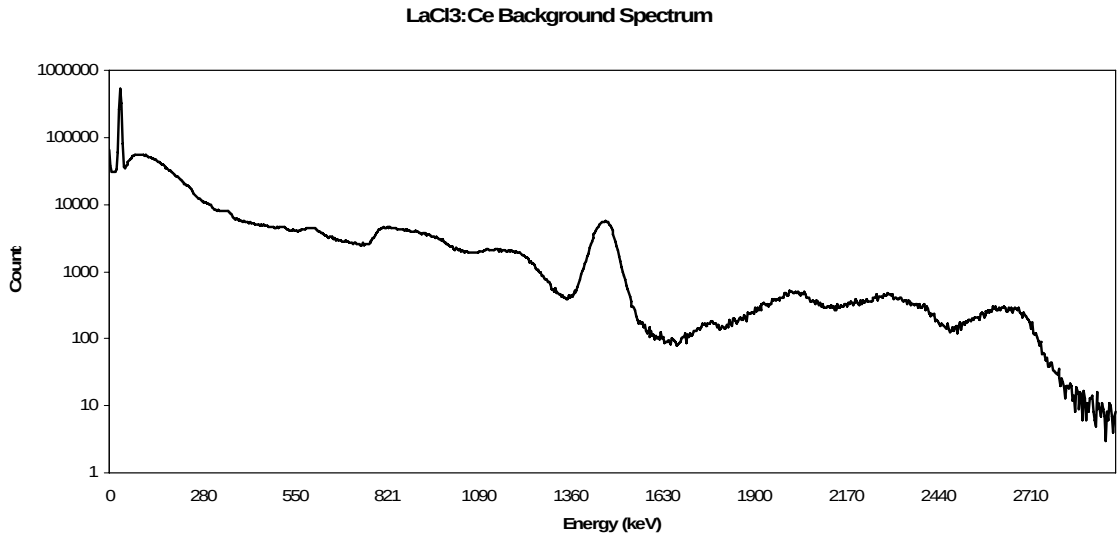

Figure 2. $LaCl_3$:Ce background spectrum (50000 Seconds).

The dominant features in Figure 2 are, however, due to the internal La-138 contamination. There is an x-ray peak at approximately 32 keV. The peak in the center

of the spectrum is at about 1468 keV. It is the 1436-kev gamma ray plus the coincident x-ray. The broad feature at 750-1000 keV is the 789-keV gamma ray in coincidence with a beta particle. The net count rates for the x-ray peak, the 789-kev gamma-plus-beta hump, and the 1468-kev gamma-plus-x-ray peak are 23.8, 2.1, and 2.3 counts/s, respectively. The small bumps between 250-650 keV are background gamma rays, such as the 609-kev and 352-keV gamma rays from the U-238 decay chain.

Figure 3 shows a coincidence spectrum taken with the same $LaCl_3$:Ce crystal operated in coincidence with an adjacent 9.67 cm long by 9.17 cm diameter cylindrical 120% ORTEC [12] p-type HPGe detector. A XIA DGF-4C digital pulse processor [13] was used as the digital pulse processing system for both spectrometers. Figure 3 plots all coincident events within a 4 μs gate collected over 13197 seconds (live-time). Both axes are labeled in gamma-ray calibrated energy units. The outer diagonal line running from above 1400 keV from one axis to the other represents total energy collection of the 1435.8-keV La-138 gamma ray (plus coincident x-ray) in the two detectors. The vertical band at low $LaCl_3$:Ce energies, and below the intense HPGe horizontal stripe at 1435.8 keV of deposited energy, is due to the capture of the low-energy x-rays in the $LaCl_3$:Ce in coincidence with some signal in the HPGe detector.

Detection of the 1435.8-keV and 788.7-keV gamma rays by the HPGe is clearly shown by horizontal lines. These gamma rays are detected in coincidence with x-rays and betas, respectively, in the $LaCl_3$:Ce detector. The broad vertical band below the 788.7-keV gamma ray in the HPGe detector is due to partial energy detection by the HPGe detector

in coincidence with the betas in the $LaCl_3$:Ce detector. The band is broad due to the range of beta energies (0-255 keV). This causes the diagonal line associated with the deposition of the 788.7-keV gamma ray in both detectors to be broadened also. Figure 3 also reveals a faint diagonal line between those of the 788.7-keV and 1435.8-keV gamma rays. This is due to situations where the 1435.8-keV gamma ray Compton-scattered in both detectors and the residual gamma ray escaped.

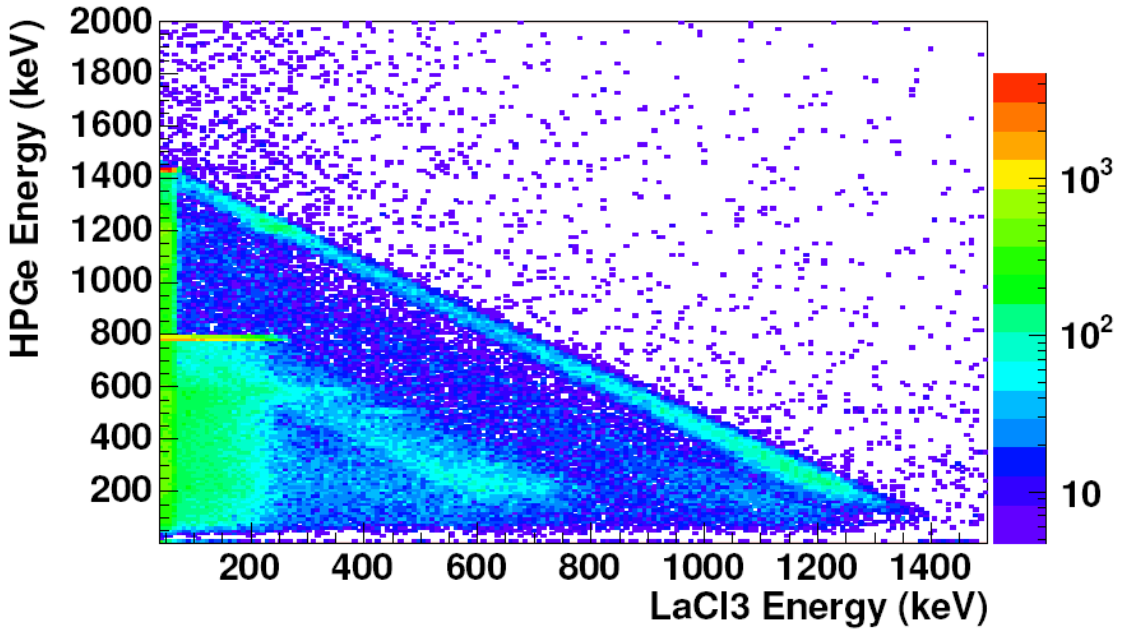

Figure 3. Coincidence spectrum of LaCl3:Ce scintillator and HPGe detector. Color represents the number of counts.

Observations

It is unfortunate that one of the most-promising new scintillator materials in years (in terms of resolution) has a naturally-occurring radioisotope. We note that the other main lanthanide generating substantial interest for scintillators materials, lutetium, also has a naturally-occurring isotope, Lu-176, with an even higher natural abundance (2.5%). The presence of these naturally-occurring radioisotopes presents more of a problem for some

applications (such as low-background measurements) than others (such as medical imaging, where the fast signals of the lanthanide halides is particularly appealing). One particular problem the 1468-kev gamma-plus-x-ray peak from the naturally-occurring La-138 causes for lanthanum halide scintillators is its interference with the K-40 1460.8-keV gamma ray prominently found in natural background. Our MCNPx simulation of the $LaCl_3$:Ce crystal whose background spectrum is displayed in Figure 2 successfully approximated the observed gross count rate of the 1468-kev gamma-plus-x-ray peak and attributed only 70% of the gross counts to the La-138 The other 30% of the counts were due to the natural background – a combination of K-40's 1460.8-keV gamma ray plus Compton-continuum gamma rays from higher-energy gamma rays also found in the natural background. Many materials of commercial interest, such as fertilizer, ice melt, and tile, due to their K-40 concentrations, have significantly enhanced radioactivity relative to the natural background, however. Thus handheld Radio-Isotope Identification Devices (RIIDs) are often asked to identify K-40 as a source of radiation [14]. For this application, then, the effects of the La-138 will need to be investigated [15]. On a positive note, it may be possible to devise a system for self-calibration of lanthanum halide-based detectors using the gamma rays from the La-138.

Nonetheless, the La-138 count rates are not necessarily so high as to mitigate the detector's usefulness for traditional isotope identification purposes. Figure 4 shows a 5000-second spectrum of a single Thoriated lantern mantle (containing Th-232) placed in contact with the $LaCl_3$:Ce crystal. Such mantles are not particularly radioactive (containing ~300 mg of Th) but the spectrum is well resolved, in spite of the presence of

the La-138 x-ray and 1468-keV peaks. Note the separation of the 911-keV and 969-keV gamma rays. NaI(Tl)'s resolution does not allow this separation, nor does it so clearly delineate the many minor gamma-rays present in this spectrum, such as the 129-keV, 209-keV, 463-keV, and many other gamma rays. Clearly, it will have to be determined for individual applications, based on the activities that are expected to be measured, whether or not lanthanum halide detectors are a beneficial replacement for NaI(Tl).

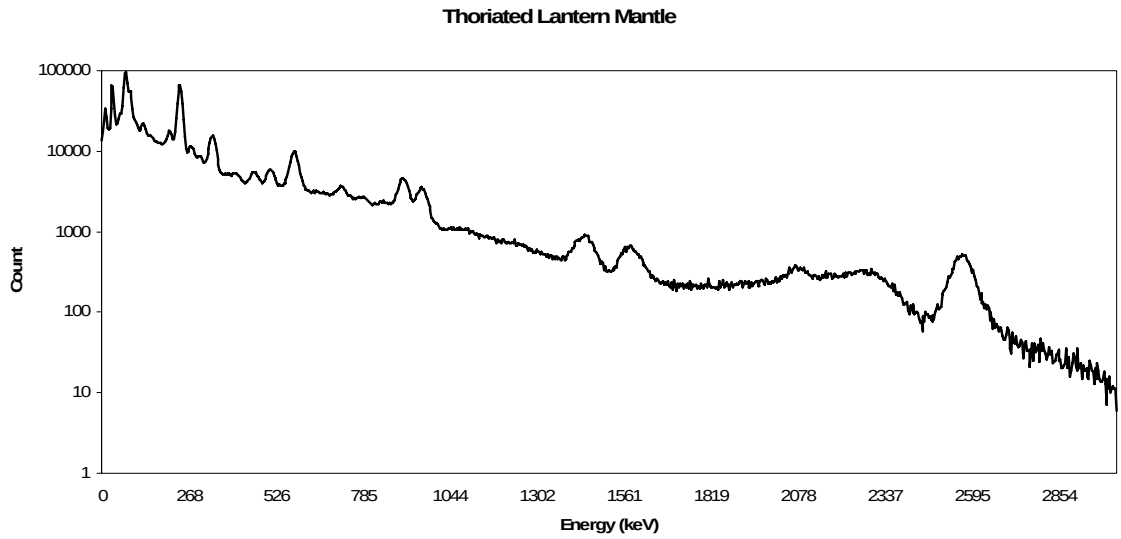

Figure 4. 5000 second spectrum of one thoriated lantern mantle.

High Neutron Flux Study

We also briefly investigated the performance of $LaCl_3$:Ce in neutron fields. Lanthanum halides' short decay times make it attractive, from a count-rate perspective, in high-count rate applications like nuclear reactor spent fuel assay. However, the fact that isotopes of lanthanum and chlorine have neutron interaction cross-sections that may lead to unacceptably high background rates and interferences in neutron fields needs to be

explored. One such investigation follows, but more detailed study will be needed prior to actual application.

A 25 mm x 25 mm right cylinder was exposed for one week next to a PuBe neutron source whose flux is 8.8 x 10^9 neutrons/second. La-139 has a thermal neutron cross section of 9.0 barns [16]. La-140 has a 1.6780 day half-life and beta-decays to stable Ce-140 [5]. After the neutron exposure, the crystal had become activated to the extent that its background spectrum was now overwhelmed by internal betas. Figure 5 shows a 30000 second background spectrum taken one week after the activation. The energy scale is based on the detector's response to gamma rays under identical conditions prior to its exposure. The detector's count rate for energies above the low-energy x-ray was 185 counts/sec, 9.4 times that of the count rate for the same region before the detector was activated. Figure 6 shows a spectrum taken with the coincidence detector setup described earlier. It displays what the HPGe detector detected, when it was in coincidence with the $LaCl_3$:Ce scintillator. The spectrum was taken for 22208 seconds (real-time), beginning approximately 5 hours after the scintillator was removed from activation. All of the peaks shown, except for an unidentified peak at 2754 keV, are attributable to La-140. (Some represent coincident gamma rays rather than single gamma rays.) Had the spectrum been taken sooner after activation, it is probable that Cl-38 (half-life: 37.2 minutes) gamma rays would also have been seen. These results imply that it will be necessary to shield the $LaCl_3$:Ce detector from thermal neutrons with Cd in high neutron fields.

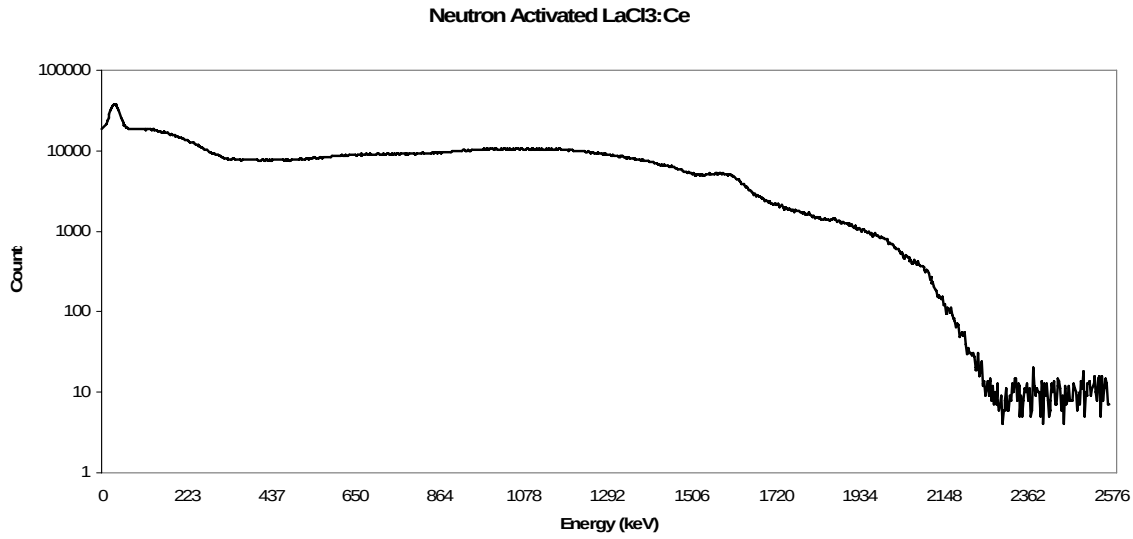

Figure 5. Background spectrum of neutron activated $LaCl_3$:Ce crystal, one week after activation.

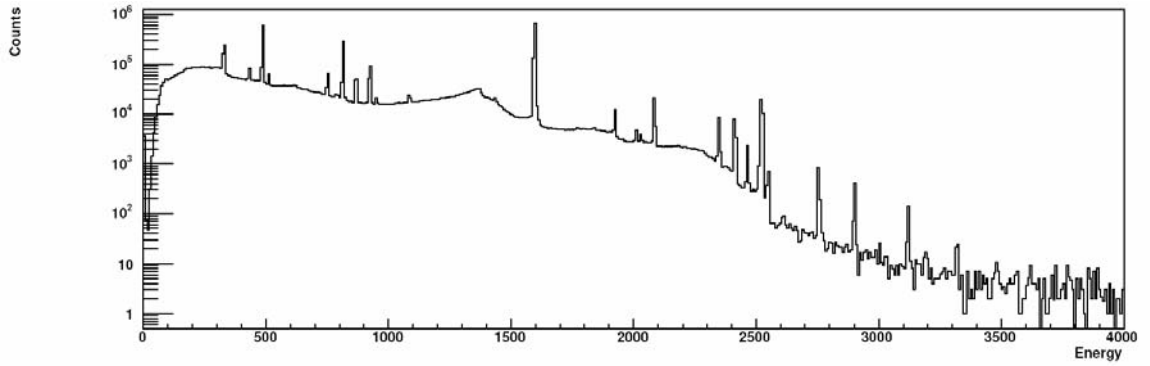

Figure 6. HPGe spectrum of activated $LaCl_3$:Ce crystal, gated on coincident signal with crystal.

Conclusion

The reduction of alpha-contamination (due to Ac-227) in lanthanum halide scintillators by two orders of magnitude since previous studies were conducted a year earlier is encouraging. However, as the crystal size has grown, the effects of the high-energy gamma decay products of the naturally-occurring radioisotope La-138 are more pronounced and the performance penalty of that natural (and unavoidable) contaminant needs to be understood in different applications. La-138 produces x-rays, gamma rays, and beta particles that affect the low-count spectra of lanthanum halide scintillators.

Thus, in spite of the greatly improved resolution (4.4% at 662 keV for our $LaCl_3$:Ce scintillator), it will have to be determined on a case-by-case basis whether lanthanum halides are suitable replacements for NaI(Tl) detectors. La-139's cross-section may also limit the detector's usefulness in high neutron field situations, due to the potential for activation.

Acknowledgement

The authors appreciate the help of Walt Hensley (PNNL) for running relevant MCNPx simulations for this study.

REFERENCES

[1] B.D. Milbrath, R.C. Runkle, T.W. Hossbach, W.R. Kaye, E.A. Lepel, B.S. McDonald, L.E. Smith, Nucl. Inst. Meth. A **547**, 504 (2005); PNNL-SA-42859.

[2] J.K. Hartwell, R.J. Gehrke, App. Rad. Iso. **63** 223 (2005).

[3] A. Iltis, G. Gautier, J.F. Nee, P. Raby, IEEE/NSS-MIC 2004, Rome, Italy, Oct. 16-22, 2004.

[4] M. Balcerzyk, M. Moszynski, M. Kapusta, Nucl. Inst. Meth. A **537**, 50 (2005).

[5] Saint-Gobain Crystals and Detectors, 12345 Kinsman Road, Newberry, OH 44065, USA.

[6] R.B. Firestone, S.Y.F. Chu, C.M. Baglin, Table of Isotopes CD_ROM, eight ed, Wiley, New York, 1999; R.B. Firestone and L.P. Ekstrom, WWW Table of Radioactive Isotopes, Version 2.1, January 2004, http://ie.lbl.gov/toi/index.asp.

[7] C.W.E. van Eijk, Nucl. Inst. Meth. A **471**, 244 (2001).

[8] E.V.D. van Loef, P. Dorenbos, C.W.E. van Eijk, K. Krämer, H.U. Güdel, IEEE Trans. Nucl. Sci. **48**(3), 341 (2001).

[9] K.S. Shah, J. Glodo, M. Klugerman, L. Cirignano, W.W. Moses, S.E. Derenzo, M.J. Weber, Nucl. Inst. Meth. A **505**, 76 (2003).

[10] Saint-Gobain Crystals and Detectors, 12345 Kinsman Road, Newberry, OH 44065, USA.

[11] D.B. Pelowitz, ed., *MCNPx User's Manual*, LA-CP-05-0369, Los Alamos National Laboratory, Los Alamos, NM , 2005.

[12] ORTEC, 801 S. Illinois Ave., Oak Ridge, TN 37831, USA.

[13] X-ray Instruments Associates, 8450 Central Ave., Newark, CA 94560, USA.

[14] D. Bates and M. Woodring, *Initial Metadata Analysis for Northern Border Ports of Entry*, PNNL-14757, Pacific Northwest National Laboratory, Richland, WA 99352 (2004).

[15] B.D. Milbrath, B.J. Choate, R.L. Kouzes, J.E. Schweppe, IEEE/NSS-MIC 2005 Conference, Fajardo, Puerto Rico, Oct. 23-29, 2005.

[16] E.M. Baum, H.D. Knox, T.R. Miller, Nuclides and Isotopes, 16th Edition, Knolls Atomic Power Laboratory.